Paper

Identification of Background in CMA

Adel Alkafri,[a] K. Goto,[b,*] Y. Ichikawa,[a] and R. Shimizu[c]
[a]*Nagoya Institute of Technology (NIT); Gokiso-cho; Showa-ku, Nagoya 466-8555*
[b]*Advanced Industrial Science and Technology (AIST); 2266-98 Shimoshidami; Moriyama-ku, Nagoya 463-8560*
[c]*Osaka Institute of Technology (OIT); 1-79-1 Kitayama; Hirakata 573-0196*
[*]*gotou.keisuke@aist.go.jp*

(Received: January 17, 2007; June: 11, 2007)

We studied the background in electron spectroscopy that was caused by the scattering of signal electrons in the specific cylindrical mirror analyzer (CMA) developed for absolute Auger electron spectroscopy. For this, a mini-electron gun was set at a sample position to calibrate the trajectories of signal electrons in the CMA. The electron beam current (i_{in}) entering the CMA was measured using a retractable Faraday cup and the detected current (i_{out}) was measured using another Faraday cup (normally used for detecting Auger electrons). It was revealed that the two meshes spun in the inner cylindrical electrode act as micro lenses for signal electrons, significantly deteriorating the CMA characteristics by the deflection and scattering of the signal electrons in the CMA. The measured energy spectra demonstrated the excellent performance of electron spectrometry with a dynamic range of ~10^7.

1. Introduction

Sophisticated instruments capable of use for Auger electron spectroscopy (AES) and X-ray photoelectron spectroscopy (XPS) are produced by many manufacturers and are widely distributed and in regular use [1-3]. However, the spectra obtained include some uncertainty regarding the absolute intensities and energy positions of the measured peaks. Activity within the **ISO** Technical Committee 201 (Surface Chemical Analysis) [4-7] introduced the use of the **SI** (International System of Units) in the field of Surface Chemical Analysis and electron spectroscopy [8,9]. The Versailles Project on Advanced Materials and Standards-Surface Chemical Analysis (VAMAS-SCA) activity [10-12] is closely related to standards developed by ISO/TC201 on surface chemical analysis.

In addition, the transmission and the contribution of the instruments to the background in the spectra are also important issues for electron energy analyzers. These significant factors are, however, very difficult to assess and reduce [13-20]. Example spectra of AES by the CMA available from the COMPRO program in the Surface Analysis Society of Japan (SASJ) [21] have revealed that experimental spectra include some unresolved features due to the finite energy resolution of the analyzer used [22-23].

The present work aims at examining the formation of the background in the CMA to better understand the details of the spectra. For this, we set up a mini-electron gun at the sample position to calibrate the trajectories of signal electrons in the CMA by measuring the electron beam current (i_{in}) with a retractable Faraday cup and the detected current (i_{out}) with another Faraday cup (normally used for detecting Auger electrons). Sophisticated detection equipment, for the measurement of the absolute intensity of electron beam current, enabled electron spectroscopy with a dynamic range, ~10^7, revealing details of the background formation caused by the deflection and scattering of signal electrons in the CMA.

2. Experimental

Figure 1 is a schematic diagram of the CMA used for transmission measurement [24,25]. A mini-electron gun was set at the sample position. This electron gun consists of a ball (0.3 mm in diameter) point tungsten hairpin filament and Wehnelt electrode, providing an electron beam of primary energy from 1 eV to 3 keV. The emission current was measured using an extractable Faraday

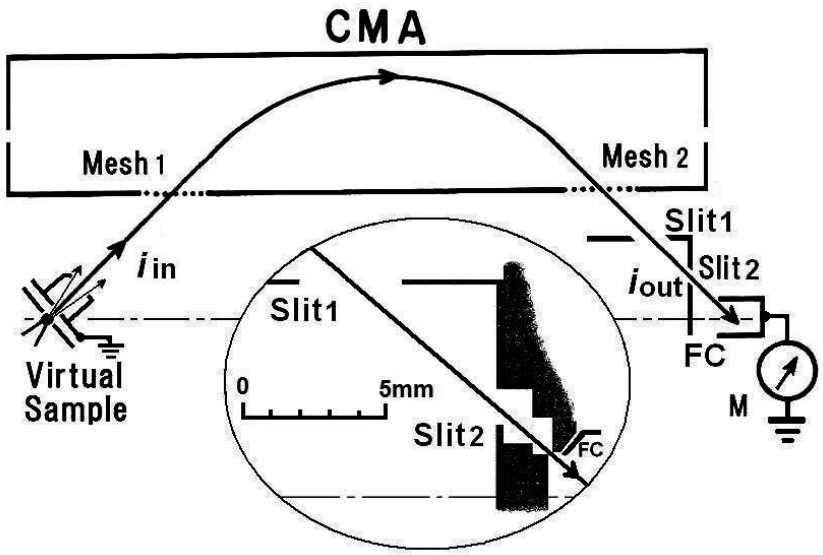

Fig. 1. Schematic experimental set up. Inset is detail of **Slit$_2$**.

cup (not shown here) revealing the stability to be better than 1% during the experiment. The emission angle was so strictly confined to a cone of 42.3°±6°, which means only 4% of the emission current entered into the CMA. A similar electron gun has been used in Ref. [26]. The internal focusing of such an electron gun means that the electron trajectories may not be simply radial and in practical analysis, we need to confirm that the electron beam would fill the acceptance area of the CMA, which might be azimuthally dependent [27]. We cannot apply any method to study the whole acceptance area, because the mini-electron gun was rigidly fastened at the calculated position. We did an experiment as like as in an actual experiment by using a known mesh. It is easy to identify the beam position by counting the steps and intensity of the emission pattern using a fluorescent screen behind the mesh (not shown) [25]. The screen was taken out after the confirmation. We used the Wehnelt bias of zero and considered it might be the optimum.

The electrons that passed through the CMA were measured with another Faraday cup (**FC**) connected to an electrometer (**M**, Keithley 642LN) to be detected as i_{out}. This detection system is normally used for AES. Two meshes (**Mesh$_1$** and **Mesh$_2$**) were set to ensure that the electric field was close to the theoretical logarithmic field. The meshes were made of 100-mesh woven gold-plated tungsten wire on which Aquadag® (carbon composite) and soot (carbon) were coated to reduce the number of secondary electrons emitted and electron scattering on the meshes. Another advantage of the coating is that the carbon is quite effective in stabilizing the work function of the mesh surface [28].

The inset in Fig. 1 shows the detail of the slits (**Slit$_1$** and **Slit$_2$**). **Slit$_1$** roughly limited the number of unwanted electrons coming to **Slit$_2$** [20]. **Slit$_2$** determines the energy resolution of the CMA. In the present measurement, 183 μm was adopted as the smallest width (calculated). The rather complicated structure of **Slit$_2$**, set just in front of the Faraday cup (**FC**), was mainly due to the intention to prevent secondary and scattered electrons from reaching the Faraday cup. All construction was rigid, *i.e.*, non-adjustable from the outside, since misalignment of the system would easily lead to deterioration of the performance of the CMA. Fortunately, it seems that this problem has not occurred. The CMA system was evacuated by a turbo molecular pump and a sputter ion pump but was not backed. The vacuum was, therefore, in the low 10^{-5} Pa throughout the measurements. We considered that the vacuum was good enough for the present experiments.

3. Experimental results and discussion

To study the transmission, we measured the total energy distribution of the transmitted electrons and examined the intensity (current), position, and shape of the main peak. The obtained spectra are shown in Fig. 2 for accelerating voltages of the primary electrons from 250 V to 3 kV and for 1 V to 100 V in Fig. 3. These spectra

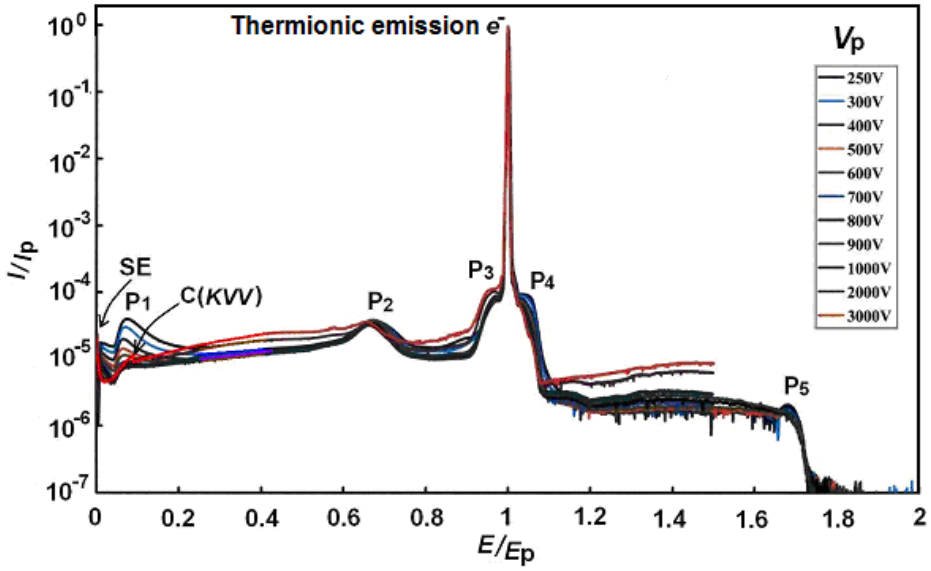

Fig. 2. Normalized total energy spectra of the thermionic emission accelerated by 250 V through 3000 V that accompanied the broad range of the so-called background.

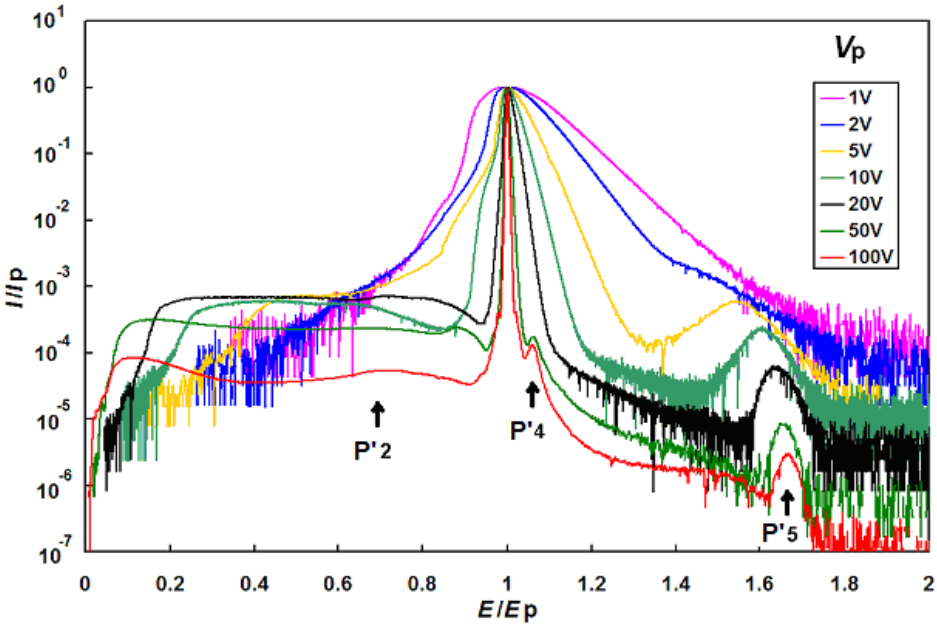

Fig. 3. Normalized total energy spectra of the thermionic emission accelerated by 1 V through 100 V that accompanied the broad range of the so-called background. Primed peaks correspond to those in Fig. 2.

were normalized to the peak intensity (I_p) and primary energies (E_p), respectively. In both figures, it should be noted that each main peak is associated with particular peaks, *i.e.*, **SE**, $\mathbf{P_1}$, $\mathbf{P_2}$, $\mathbf{P_3}$, $\mathbf{P_4}$, and $\mathbf{P_5}$. These particular peaks are considered to be largely due to the geometry of the CMA. We can account for the structures by estimating the electron trajectories that could come from the construction of the CMA.

The estimated traces for these peaks are shown in Fig. 4. When an electron impinges on the electrode surface, it causes secondary electron emission and electron scattering. Since the electron trajectories in a CMA can be calculated with considerable accuracy [26,29], the complicated spectra in Figs. 2 and 3 can also be analyzed. **SE** represents the secondary and scattered electrons generated at the outer cylindrical electrode. Since, in this case,

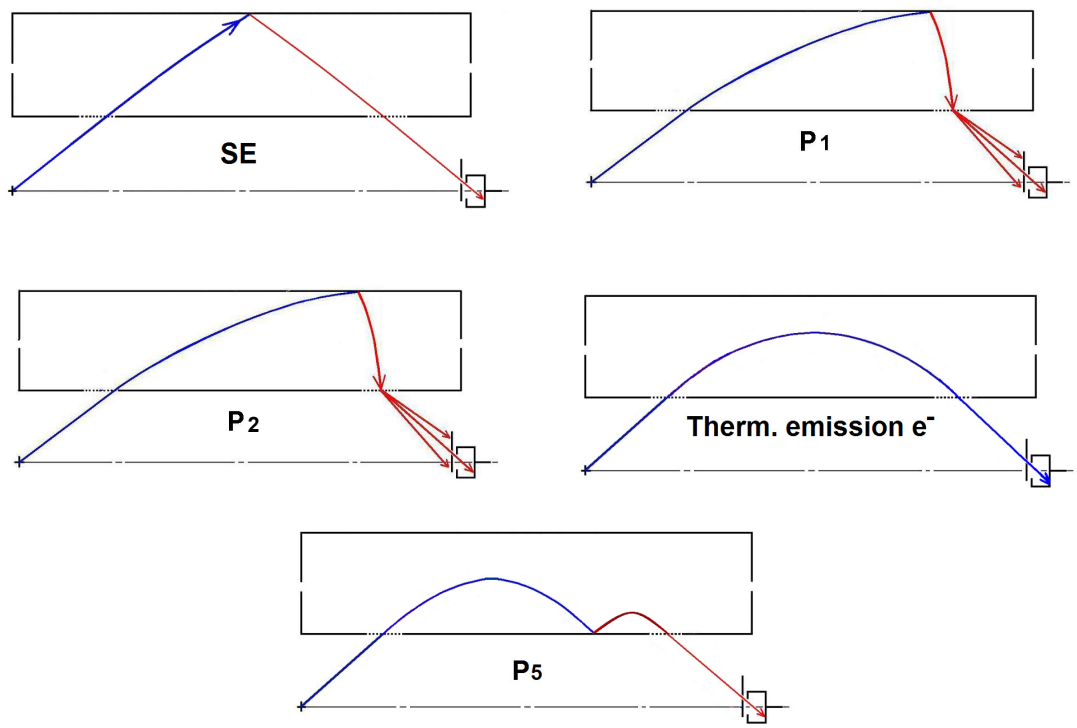

Fig. 4. Possible mechanisms of spectrum-like structures in the background; **SE**, $\mathbf{P_1}$, $\mathbf{P_2}$, e^-, and $\mathbf{P_5}$ in Fig. 2.

a very weak electric field close to zero was supplied to the outer cylindrical electrode, those secondary and scattered electrons travel into the **FC** along nearly straight trajectories like a mirror.

These electrons can be reduced to some extent by setting the ratio of the radius of the outer cylinder to that of the inner cylinder to be larger than 3.4 [23]. $\mathbf{P_1}$ indicates secondary electrons generated at $\mathbf{Mesh_2}$ by the scattered electrons from the outer cylindrical electrode. $\mathbf{P_2}$ was caused by a mechanism similar to $\mathbf{P_1}$, but the primary electrons were scattered at the end of the fringe of the inner or outer cylindrical electrode. The flat distribution extending from $\mathbf{P_4}$ to $\mathbf{P_5}$ is attributed to those electrons that were once scattered at the inner cylinder and hopped into the **FC** [14,15,20]. The lower the primary energy, the more $\mathbf{P_5}$ is pronounced, as seen in Figs. 2 and 3. This is primarily because the yield of the elastically backscattered electrons increases for a lower primary energy. This tendency, however, becomes rather vague for primary energies below 5 eV where the hopping electrons are buried under the Boltzmann tail of the thermionic emission. No further hopping was of the electrometer observed beyond $\mathbf{P_5}$, where only residual electronic noise was found. The $\mathbf{P_5}$ was the scattered almost the elastic reflection of thermionic emission e^- and the intensity was already about 10^{-5} of the original one. The strong retarding electric field in the CMA at $\mathbf{P_5}$ would return any scattered and secondary electrons to the inner cylinder and they were absorbed. The $\mathbf{P_5}$ with almost the primary electrons could hop to the higher energy position, but the intensity might be orders of magnitude less than $\mathbf{P_5}$, which is far below the noise. Note that the noise level beyond $\mathbf{P_5}$ clearly indicates that the dynamic range in the spectra reaches as high as ~10^7.

The detail of the profile of the main peak for a primary energy of ~3 keV is shown in Fig. 5. The structures between $\mathbf{P_3}$ and $\mathbf{P_4}$ were identified by taking into account, not only the geometries of $\mathbf{Mesh_2}$, $\mathbf{Slit_1}$, and $\mathbf{Slit_2}$, but also the lens effect of $\mathbf{Mesh_1}$. Since $\mathbf{Mesh_1}$ acts as a weak concave lens due to the immersing electric field through the mesh hole, primary electrons, which passed through $\mathbf{Mesh_1}$, undergo deflection (divergence). Their trajectories are indicated by red lines (with arrows) in **a** and **a**' in Fig. 5. The amount of these deflected electrons reaches about 1~10% of the main peak height (e^-). The secondary and scattered electrons generated at $\mathbf{Slit_2}$ by normal and deflected primary electrons are indicated by **b** and **b**'. The flat regions at $\mathbf{P_3}$ and $\mathbf{P_4}$ are caused by the secondary and scattered electrons from $\mathbf{Mesh_2}$.

Assuming thermionic emission as having the shape of a Gaussian peak and a cathode temperature T= 2043 K, we estimated the FWHM of the energy distribution of the

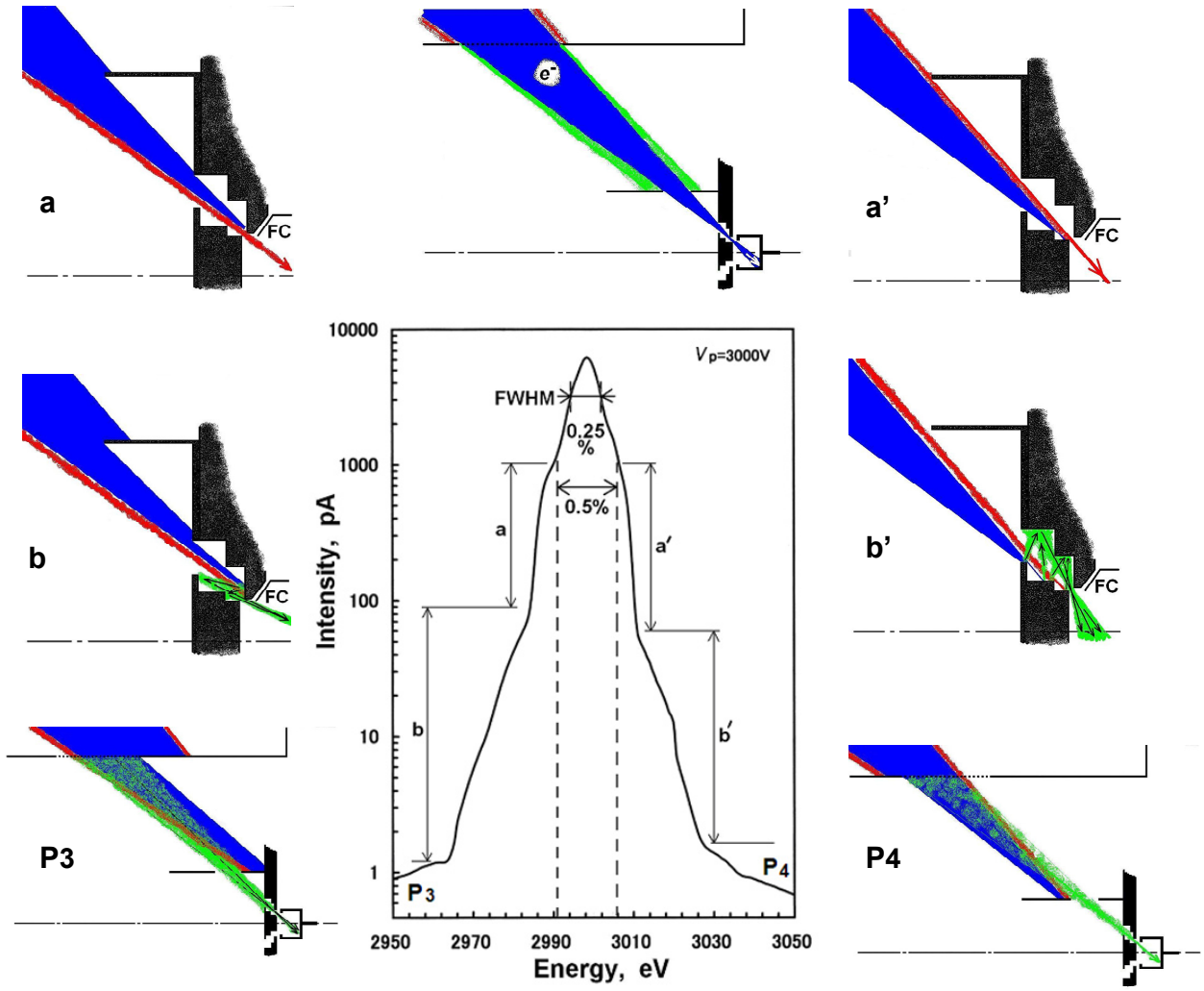

Fig. 5. Details of thermionic emission around the main peak. Possible mechanisms for the structure of the energy spectra are shown as $\mathbf{P_3}$, **a**, **a**', **b**, **b**', and $\mathbf{P_4}$.

primary electron beam to compare with the experiment. The calculation provided a good agreement with the results of the present beam measurement in the energy distribution down to the FWHM. Below the FWHM, however, the shape of the experimental peak becomes broader than the calculated one. This tendency is common for accelerating voltages below ~3 kV, as seen in Fig. 6. If a finer mesh, which should cause a weaker lens effect, is used for $\mathbf{Mesh_1}$, one could expect better agreement between the shapes of the experimental and calculated peaks even below FWHM. The effect of the finer mesh would, however, be only relevant for the regions **a** and **a**' in Fig. 6. The meshes used in the present CMA are 100-mesh (wire–to-wire spacing is 254 μm and wire diameter is 27 μm). Consequently, there still remains further improvement by using a finer mesh.

In Fig. 7, a peak that is small but distinct appears at 270 eV. This peak was observed for primary energies higher than 500 eV and is an additional evidence of the primary electrons that were once scattered at the mesh ($\mathbf{Mesh_1}$) wires, exciting carbon *K*-ionization and finally resulting in carbon ***KVV*** Auger electrons going into **FC**. This peak is found in Fig.2, as well.

4. Conclusion

The transmission characteristics of our CMA were measured using a mini-electron gun to obtain information on the so-called, background. It is necessary to characterize the background for an assessment of signal spectra. Down to 1 eV, the determined transmission was similar to that expected from theoretical estimation based on the assumption that the shape of the thermionic emis-

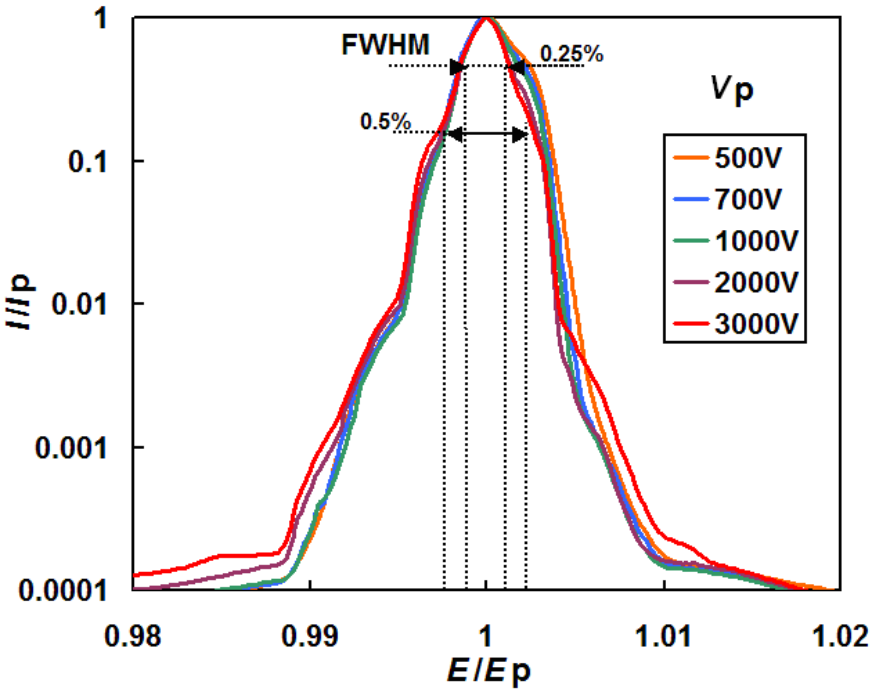

Fig. 6. Details around the main peak of thermionically emitted electrons at acceleration voltages of 500 V through 3000 V. Dotted lines indicate the theoretical calculated energy resolutions of 0.25% (FWHM) and 0.5% (full width).

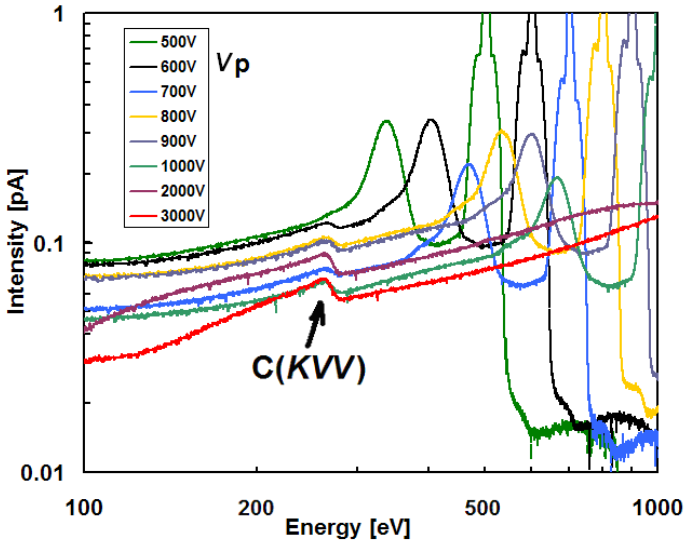

Fig. 7. Energy spectra for acceleration voltages of 500 V through 3000 V; partial plot of Fig. 2 using an energy scale. Carbon Auger electrons, **C**(***KVV***), at about 270 eV from **Mesh$_1$** can be seen.

sion from the ball-pointed W-filament was a Maxwell-Boltzmann energy distribution for a filament temperature T= 2043 K. Simulations of electron trajectories from the electron gun to the detector (Faraday cup) via the CMA revealed that secondary electrons generated at the two meshes (at the entrance and exit of the CMA) and scattering of primary electrons on the surfaces of the inner and outer cylindrical electrodes are the main factors in the formation of the background. Furthermore, weak lens action (concave) caused by the entrance mesh (**Mesh$_1$**) also caused a broadening of the primary electron peak. The shape of the **Slit$_2$** in front of the Faraday cup (**FC**) might affect the background. In the present experiment, improvements and careful maintenance of

the high voltage power supply (John-Fluke, 408B), by replacing the electronic parts with an up-to-date IC and zener diodes, combined with a precision high voltage divider and an electrometer (Keithley, 642LN), have enabled the achievement of high energy resolution and dynamic range as high as ~10^7.

5. Acknowledgements

The Special Coordinated Research of Science and Technology through NIMS have supported the work. We would like to express our gratitude to the members of SASJ for their helpful comments and encouragement for this work. Dr. S. Ichimura, Dr. Y. Yamauchi and Ms Y. Shoji in AIST encouraged K.G. to perform the work. One of the authors (A.A.) would like to express his gratitude to the Japanese Ministry of Education, Culture, Sports, Science and Technology for a scholarship.

6. References

[1] K. D. Childs, B. A. Carlson, L. A. LaVanier, J. F. Moulder, D. F. Paul, W. F. Stickle, and D. G. Watson, *Handbook of Auger Electron Spectroscopy*, 3rd edition, Physical Electronics Industries (1994).

[2] *Auger Electron Spectra Catalogue*, ANELVA corporation (1979).

[3] T. Sekine, Y. Nagasawa, M. Kudoh, Y. Sakai, A. S. Parkes, D. J. Geller, A. Mogami, and K. Hirata, *Handbook of Auger Electron Spectroscopy*, JEOL (1982.).

[4] M. P. Seah, *J. Electron Spectrosc. Relat. Phenom.* **97**, 235 (1998).

[5] M. P. Seah and G. C. Smith, *Surf. Interface Anal.* **15**, 751 (1990).

[6] G. C. Smith and M. P. Seah, *Surf. Interface Anal.* **16**, 144 (1990).

[7] M. P. Seah, *J. Electron Spectrosc. Relat. Phenom.* **71**, 191 (1995).

[8] R. Shimizu, *J. Vacuum Society of Japan* **30**, 666 (1987) (*in Japanese*).

[9] K. Yoshihara, S. Ichimura, Y. Furukawa, M. Suzuki, S. Hashimoto, S. Tanuma, Y. Honma, *J. Surface Sci. Society of Japan*, **24**, 201 (2003) (*in Japanese*): S. Ichimura *et. al.*, *表面化学分析技術・マイクロビーム分析技術　国際標準化活動状況* (*Surface Chemical Analysis Technology, Microbeam Analysis Technology, Recent Report on International Standardization Activity*), JSCA News Special Issue, Standardization Society of Japan (2006/09/01).

[10] C. J. Powell, N. E. Erickson, and T. E. Madey, *J. Electron Spectrosc. Relat. Phenom.* **25**, 87 (1982).

[11] C. J. Powell and M. P. Seah, *J. Vac. Sci. Technol.* **A 8**, 735 (1990).

[12] M. P. Seah and G.. C. Smith, *Surf. Interface. Anal.* **17**, 855 (1991).

[13] H. Ehrhart, L. Langhans, F. Linder, and H. S. Taylor, *Phys. Rev.* **173**, 222 (1968).

[14] H. Froitzheim. H. Ibach, and S. Lehwald, *Rev. Sci. Instrum.* **46**, 1325 (1975).

[15] C. B. Bargeron and B. H. Nall, *Rev. Sci. Instrum.* **52**, 1777 (1981).

[16] M. P. Seah, *Surf. Interface Anal.* **20**, 865 (1993).

[17] M. P. Seah, *Surf. Interface Anal.* **20**, 876 (1993).

[18] J. C. Greenwood *et al.*, *Surf. Interface Anal.* **20**, 8891 (1993).

[19] M. M. El Gomati and T. A. El Bakush, *Surf. Interface Anal.* **24**, 152 (1996).

[20] N. Nissa Rahman, K. Goto, and R. Shimizu, *J. Surface Anal.* **8**, 2 (2001).

[21] http://www.sasj.jp/COMPRO/index.html.

[22] K. Goto, *J. Surface Anal.* **9**, 18 (2002).

[23] K. Goto, N. Sakakibara, and Y. Sakai, *Microbeam Anal.* **2**, 123 (1993).

[24] K. Goto, Adel Alkafri, Y. Ichikawa, and R. Shimizu, *J. Surface Sci. Society of Japan*, **27**, 649 (2006) (*in Japanese*).

[25] Adel Alkafri, Y. Ichikawa, R. Shimizu, and K. Goto, *J. Surface Anal.* **14**, (2007).

[26] H. Z. Sar-El, *Rev. Sci. Instrum.* **38**, 1210 (1967).

[27] M. P. Seah and H. J. Mathieu, *Rev. Sci. Instrum.* **56**, 703 (1985).

[28] W. Y. Li, K. Goto, and R. Shimitzu, *Surf. Interface Anal.* **37**, 244 (2005).

[29] V. V. Zashkvara, M. I. Korsunski, and O. S. Kosmachev, *Sov. Phys.-Tech.Phys.* **11**, 96 (1966).

Discussion between referees and authors

Referee 1: Dr. M. P. Seah (NPL, UK)

This is an interesting development of the meticulous work from the CMA activity in Nagoya. The referee has some points that require attention:

[Referee1-1]

In the introduction, in relation to standard spectra, the authors should note that:

a) A basic description of how standard spectra may be used and how more such spectra may then be generated are given in *Journal of Electron Spectroscopy* **71**, 191-204 (1995), "A System for the Intensity Calibration of Electron Spectrometers" by M. P. Seah.

b) Standard spectra for AES and XPS are given in *Surface and Interface Analysis* **15**, 751-766 (1990), "Quantitative AES and XPS - Determination of the Electron Spectrometer Transmission Function and the Detector Sensitivity Energy Dependencies for the Production of True Electron Emission Spectra in AES and XPS", by M. P. Seah and G. C. Smith and *Surface and Interface Analysis* **16**, 144-148 (1990), "Standard Reference Spectra for XPS and AES - Their Derivation, Validation and Use" by G. C. Smith and M. P. Seah.

c) Papers on internal inelastic scattering of electrons in analysers are given, inter alia, in 1) *Surface and Interface Analysis* **20**, 865-875 (1993) "Scattering in Electron Spectrometers, Diagnosis and Avoidance, I: Concentric Hemispherical Analysers" by M. P. Seah, 2) *Surface and Interface Analysis* **20**, 876-890 (1993), "Scattering in Electron Spectrometers, Diagnosis of Avoidance, II: Cylindrical Mirror Analysers" by M. P. Seah, 3) *Surface and Interface Analysis* **20**, 891-900 (1993) "Internal scattering of electrons in a hemispherical electron spectrometers" by J. C. Greenwood *et al*.

[Author]

We changed and added the references according to your list of the important references.

[Referee1-2]

For quantifying the transmission of a spectrometer, a source such as that shown in Fig 1 has internal focusing so that the rays are not simply radial, as pictured from a point at the CMA focus. They may or may not fill the acceptance area of the CMA and they may or may not fill the +/-6 degrees acceptance of the spectrometer. For spectrometer transmission characterization, each of these two aspects needs separate consideration such that the source either is shown to fully fill the appropriate parameter space or, alternatively, to be well within that parameter space. To match it approximately in either (or both) parameter(s) would be the worst of all possible worlds! Additionally, any aberration caused by the cylindrical meshes for the inner cylinder slits means that the acceptance area may be azimuthally dependent (see, for example *Review of Scientific Instruments* **56**, 703-711 (1985), "A Determination of the Analysis Area of the Perkin-Elmer PHI 550 ESCA/SAM X-ray Photoelectron and Auger Electron Spectrometer", by M. P. Seah and H. J. Mathieu). This all needs consideration for characterizing spectra from a given sample when the CMA is used for generating reference spectra.

[Author]

The focusing of the mini-electron gun was very complicated, for which we made many experiments. Unfortunately we cannot decide at present which was the true profile of the thermionic emission. We have repaired and arranged the e-gun several times and the emission characteristic would change in each case. Vacuum conditions changed the characteristics as well, probably due to the change of the work function. Then we chose the zero of the Wehnelt bias might be the optimum parameter for a radial emission from the virtual cathode.

The e-beam was strictly confined in the described cone as we have confirmed with a fluorescent screen (see a photo in (JSA, Vol.14, No.1 (2007) 2-8). The e-beam was cut off by the sharp edge at the end of the field free drift tube for the confinement and electron scattering.

We did not perform the off-axis experiments as you have done for the practical analysis. We aimed only to obtain a characteristic compatible for the calculation. The rigidly fixed construction gave no possibility of off-axis experiment.

[Referee1-3]

The interpretation of P5 seems wrong. The scattered intensity should fall monotonically from the main peak at $E_p/E = 1$ to zero at $E_p/E = 1.65$, without the peak at $Ep/E = 1.65$ - what causes this peak?

[Author]

The interpretation of P5 may be adequate as other sci-

entists reported and we always observe this peak in the lower acceleration voltages where an elastic reflection is considerable. No other reason for this peak can be thought of.

[Referee1-4]

In my previous refereeing point, I distinguished between the acceptance area of the spectrometer (which is on the surface of the sample) and the angular acceptance of the spectrometer. The authors write of the "acceptance area" but the context looks as though the meaning is, in fact, the acceptance area of the entrance slit (i.e. the angular acceptance and not the acceptance area of the spectrometer). Without access to reference [25], it is not possible to verify this but the material prior to and following this sentence relate to the slit and the gun emission. It appears that the issue of the acceptance area of the CMA is not addressed.

[Author]

I apologize for my misunderstanding. We added the following sentences: …[27]. We cannot apply any method to study the acceptance area and angular acceptance, because the mini-electron gun was rigidly fasted at the position. We will do an experiment for the acceptances in an actual experiment by using a known mesh. It is easy to identify the beam position by counting the steps and intensity of the spectra.

[Referee1-5]

The cause of P5 is still unclear.

[Author]

I explained in the text about the P5 and the strong fall. We show in the attached figure for far longer sweep of energy and you will find no second hopping. See also P170 in this Journal.

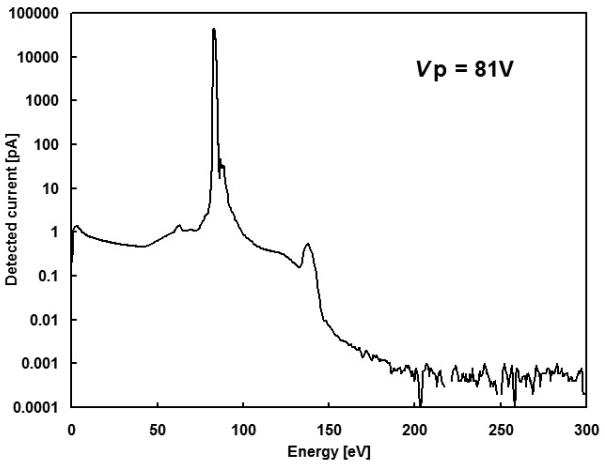

Referee 2: Dr. C. Powell (NIST, USA)

The authors present results of careful measurements to characterize the performance of their CMA. These measurements are important to others in that they show specific sources of background and scattered electrons that can occur in practice.

[Referee2-1]

The authors highlight VAMAS-SCA in their Introduction but this is inappropriate because VAMAS does not develop or publish documentary standards itself. ISO has developed such standards for AES and XPS through ISO/TC 201. The authors may be referring mainly here, however, to standard or reference spectra. Reference spectra for the calibration of the intensity scales of Auger spectrometers have already been published by Seah *et.al.* in the early 1990's (spectra for Cu, Ag, and Au). Specific reference needs to be made to this work (and not to an unpublished report by Seah [6]). Software is now available for purchase from NPL to calibrate the intensity scales of AES instruments. There are further papers by Seah describing this work, and the results of VAMAS interlaboratory tests to compare spectra on different instruments have also been published. These and similar intercomparisons for XPS have shown the existence of internal scattering in the analyzers. The authors need to refer to this earlier work and describe it appropriately.

[Author]

We changed the references accordingly. These are invaluable in AES and XPS.